12-15-2007

Demonstration of scale-down dynamic light scattering and determination of osmotic second virial coefficients for proteins

Arun Kumar Parupudi

DEMONSTRATION OF SCALE-DOWN DYNAMIC LIGHT SCATTERING AND DETERMINATION OF OSMOTIC SECOND VIRIAL COEFFICIENTS FOR PROTEINS

By

Arun Kumar Parupudi

A Thesis
Submitted to the Faculty of
Mississippi State University
in Partial Fulfillment of the Requirements
for the Degree of Master of Science
in Chemistry
in the Department of Chemistry

Mississippi State, Mississippi

December 2007

DEMONSTRATION OF SCALE-DOWN DYNAMIC LIGHT SCATTERING AND DETERMINATION OF OSMOTIC SECOND VIRIAL COEFFICIENTS FOR PROTEINS

By

Arun Kumar Parupudi

Approved:

Wilbur William Wilson Professor of Biophysical Chemistry Department of Chemistry (Major Professor)	Steven Gwaltney Assistant Professor of Physical Chemistry Department of Chemistry (Committee Member)
Svein Saebo Professor of Physical Chemistry Department of Chemistry (Committee member)	Stephen Foster Associate Professor of Physical Chemistry Department of Chemistry (Graduate Coordinator)

Gary L. Myers (Interim Dean of the College of Arts and Science)

Name: Arun Kumar Parupudi

Date of Degree: December 15, 2007

Institution: Mississippi State University

Major Field: Chemistry

Major Professor: Dr. Wilson

Title of Study: DEMONSTRATION OF SCALE-DOWN DYNAMIC LIGHT SCATTERING AND DETERMINATION OF OSMOTIC SECOND VIRIAL COEFFICIENTS FOR PROTEINS

Pages in Study: 46

Candidate for Degree of Master of Science

Protein aggregation is a phenomenon that plays a major role in protein crystallization and in protein formulation. In protein crystallization, aggregation is the prerequisite step; however, in protein formulation it has to be suppressed to assure therapeutic efficacy of the product. Light scattering techniques are the most promising methods to study the hydrodynamic properties of macromolecular solutions, which directly measures protein aggregation. Unfortunately, the normal dynamic light scattering technique is regarded as expensive because of the amount of protein used for these experiments. In order to address this problem, a scale down dynamic light scattering device has been designed.

The osmotic second virial coefficient, a dilute solution parameter helps in identifying solution conditions for protein crystal growth. The second part of this thesis involves comparison of osmotic second virial coefficient (B) measurements of lysozyme

using laser light scattering techniques with B measurements of lysozyme performed using self-interaction chromatography (SIC).

DEDICATION

I would like to dedicate this research to my parents, my brother, and Dr.W.W.Wilson.

ACKNOWLEDGMENTS

My sincere gratitude to Dr. Wilson who supported me from the first day of joining his lab and to the end of my M.S degree. He has taught me so much and has encouraged me to enhance my knowledge and research skills. My sincere thanks to Maggie Corley and Kusum Verma who gave me their support. Finally, I offer thanks to God for giving me the opportunity to work under Dr. Wilbur William Wilson.

TABLE OF CONTENTS

LIST OF TABLES

LIST OF FIGURES

FIGURE Page

LIST OF SYMBOLS, ABBREVATIONS AND NOMENCLATURE

B	Second virial coefficient (mol mL/g^2)
M	Molecular weight, also M_W (g/mol or Daltons)
K	Optical constant in static light scattering (cm^2 mol/g^2)
q	Scattering vector in dynamic light scattering (cm^{-1})
R_{90}	Rayleigh ratio for light scattering (cm^{-1})
SLS	Static light scattering
SD/SLS	Scale down static light scattering
DLS	Dynamic light scattering
D	Diffusion coefficient (cm^2/sec)
Γ	Decay constant (sec^{-1})
R_H	Hydrodynamic radius (nm)
θ	Scattering angle
dn/dc	Refractive index increment (mL/g)
K_D	Diffusion virial coefficient (mL/g)

CHAPTER I

MOTIVATION

The most daunting challenge in the biopharmaceutical pipeline is identifying protein-protein and protein-solvent interactions in various solution conditions. The ability to identify these solution conditions has relied on luck as they are approached by trial and error methods, i.e. screening various solutions. The osmotic second virial coefficient, a dilute solution parameter that reflects protein-protein interactions, has proven to be a predictor for assessment of protein self association and stabilization (1, 2, 3, 4). Assessment of self association of proteins is of primary importance in biological processes such as protein aggregation which can lead to neurological disorders (e.g. Alzheimer's and Huntington's diseases) as well as in many preformulation studies in order to increase efficacy and potency of the manufactured product. Many biophysical techniques have been developed to characterize these macromolecular pharmaceuticals such as analytical ultracentrifugation, static and dynamic light scattering, self interaction chromatography, circular dichroism, and differential scanning calorimetry (5).Among these techniques, static and dynamic light scattering methods emerged as noninvasive, efficient, and highly reliable methods to characterize proteins and to relate the osmotic second virial coefficient to the extent of the protein-protein and protein solvent interactions(1).This thesis presents 1) the demonstration and validation of a dynamic light

scattering device using a low volume flow cell to characterize macromolecules using minimal protein volume, 2) the measurement of osmotic second virial coefficients of lysozyme for the validation of self interaction chromatographic (SIC) experiments.

CHAPTER II

INTRODUCTION

2.1 Historical Review

Light scattering is regarded as one of the most reliable methods for determining biophysical properties of macromolecules in solution. Lord Rayleigh reported light scattering in 1871 and stated that the intensity of the scattered light from a dilute gas (scatterer) is inversely proportional to the fourth power of wavelength (λ) of the incident light (6,7). Rayleigh light scatterers are particles having sizes much smaller than the incident light wavelength (size < $\lambda/20$) and refractive indices close to that of the solvent (6,7). Based on the magnitude of the frequency shift, three types of light scattering are reported in the literature: elastic, inelastic and quasi-elastic (7). If the frequency of the incident light is comparable to the frequency of the scattered light, it is known as elastic light scattering. Generally, elastic light scattering is a characteristic of isotropic bodies, and the information from the scattered light is used to calculate static properties such as molecular weight, radius of gyration and the osmotic second virial coefficient.

Inelastic light scattering occurs if large frequency shifts are seen between the incident and scattered light. The primary reason for inelastic light scattering is rotational and vibrational transition of the molecules. Inelastic light scattering is also referred to as Raman scattering.

Quasi-elastic light scattering mainly measures fluctuations in the intensity of the scattered light resulting from the translational and rotational diffusive motion of the particles. These intensity fluctuations are analyzed by a correlator to obtain information about the hydrodynamic radius, R_h, of the particle, the main parameter in characterizing aggregation of macromolecules in solution.

2.2 Theory of Static Light Scattering

For a single particle Lord Rayleigh showed the ratio of the intensity of scattered light to the intensity of the incident light is expressed as (6,7)

$$\frac{I_S}{I_0} = \frac{16\pi^4 \alpha^2 \sin^2\theta}{\lambda^4 r^2} \tag{1}$$

where θ is the angle between the dipole axis and the line joining the dipole to the observer, and r is the distance between the dipole and the observer. This relation shows that the intensity of the scattered light varies inverse fourth power of the wavelength. In order to find molecular properties, we must relate polarizability, α, to the molecular weight. One way to achieve this is the relationship between refractive index, n, and the polarizability.

$$n^2 = n_0^2 + 4\pi N\alpha \quad \text{(Maxwell's equation)} \tag{2}$$

where, N is the number of particles per unit volume and n_0 is the refractive index of the solvent.

Expanding n in a Taylor series in concentration, c, and neglecting the terms higher than first order in c, we can write

$$n = n_0 + (\frac{dn}{dc})c \tag{3}$$

Substituting this equation in (2) and neglecting 2nd order terms we get,

$$\alpha = \frac{cn_0\left(\frac{dn}{dc}\right)}{2\pi N} \tag{4}$$

Substituting α in equation (1) we get,

$$\frac{I_S}{I_0} = \frac{4\pi^2 c^2 (dn/dc)^2 n_0^2 \sin^2\theta}{N^2 \lambda^4 r^2} \tag{5}$$

We determine scattering per unit volume so if there are N particles per unit volume then

$$N = \frac{N_A c}{M} \tag{6}$$

where N_A is Avogadro's number and thus we can write the ratio of the intensity of the scattered light to the intensity of the incident light as

$$\frac{I_S}{I_0} = \frac{4\pi^2 Mc\ (dn/dc)^2\ n_0^2 \sin^2\theta}{N_A \lambda^4 r^2} \tag{7}$$

In light scattering experiments for non-ideal solutions, the term $\frac{I_S r^2}{I_0 \sin^2\theta}$ is generally expressed as the Rayleigh ratio, R_θ, and equation (7) is rearranged to give

$$R_\theta = \frac{I_S r^2}{I_0 \sin^2\theta} = \frac{Kc}{\frac{1}{M} + 2Bc} \tag{8}$$

Here K = optical constant and B is the second osmotic second virial coefficient.

$$K = \frac{4\pi^2 n_0^2 (dn/dc)^2}{N_A \lambda^4} \tag{9}$$

The working equation then becomes

$$\frac{Kc}{R_\theta} = \frac{1}{M_W} + 2Bc \tag{10}$$

Thus, Kc/R_θ vs. concentration is plotted to determine molecular weight and osmotic second virial coefficient (7).

2.3 Role of the Osmotic Second Virial Coefficient in Protein Formulation

Solution conditions that optimize protein crystal growth are crucial for many crystallographers involved with structure based drug design. In order to grow protein crystals, protein–protein interactions should dominate over protein -solvent interactions. But in the case of protein formulation, protein–protein interactions should clearly be suppressed (1,3,8). So in both cases protein-protein interactions dictate the final outcome. The osmotic second virial coefficient, a well known dilute solution parameter, reflects the strength of these protein -protein interactions in various solution conditions and thus is widely used in both crystallization and protein formulation sciences (9). The sign and magnitude of the osmotic second virial coefficient are related to the extent of intermolecular attractions between proteins. A positive second virial coefficient indicates protein –solvent interactions dominate over protein –protein interactions whereas negative second virial coefficient values represent domination of protein-protein interactions over protein–solvent interactions.

Wilson and his coworkers developed a crystallization slot where second virial coefficient values of many proteins in crystallization conditions were found to be between -1×10^{-4} to -8×10^{-4} mol mL g^{-2}(3,9). Many crystallographers enjoyed success using this crystallization window and reported that working outside this crystallization slot does not yield protein crystals. If osmotic second virial coefficient values of a protein are slightly positive, i.e. they fall outside the crystallization slot, then that solvent is regarded as a good solvent in a thermodynamic sense and more suitable for formulation of the protein.

2.4 Scale-Down Static Light Scattering System

Traditional methods of static light scattering allow us to measure the osmotic second virial coefficients but require about 300µl of protein per concentration measured. In order to minimize the amount of protein sample in each measurement, a scale down static light scattering (SD/SLS) approach was introduced by the Wilson laboratory. This approach relies on the delivery of both an incident laser beam for scattering and a UV beam for protein concentration into the sample cell (1µl) simultaneously (10).These simultaneous measurements showed compatible results with traditional light scattering measurements. The main advantage of this technique is to determine both light scattering intensities and concentration at the same time expending only about 10µL of protein sample per experiment. A schematic of the system is shown in Figure 1.

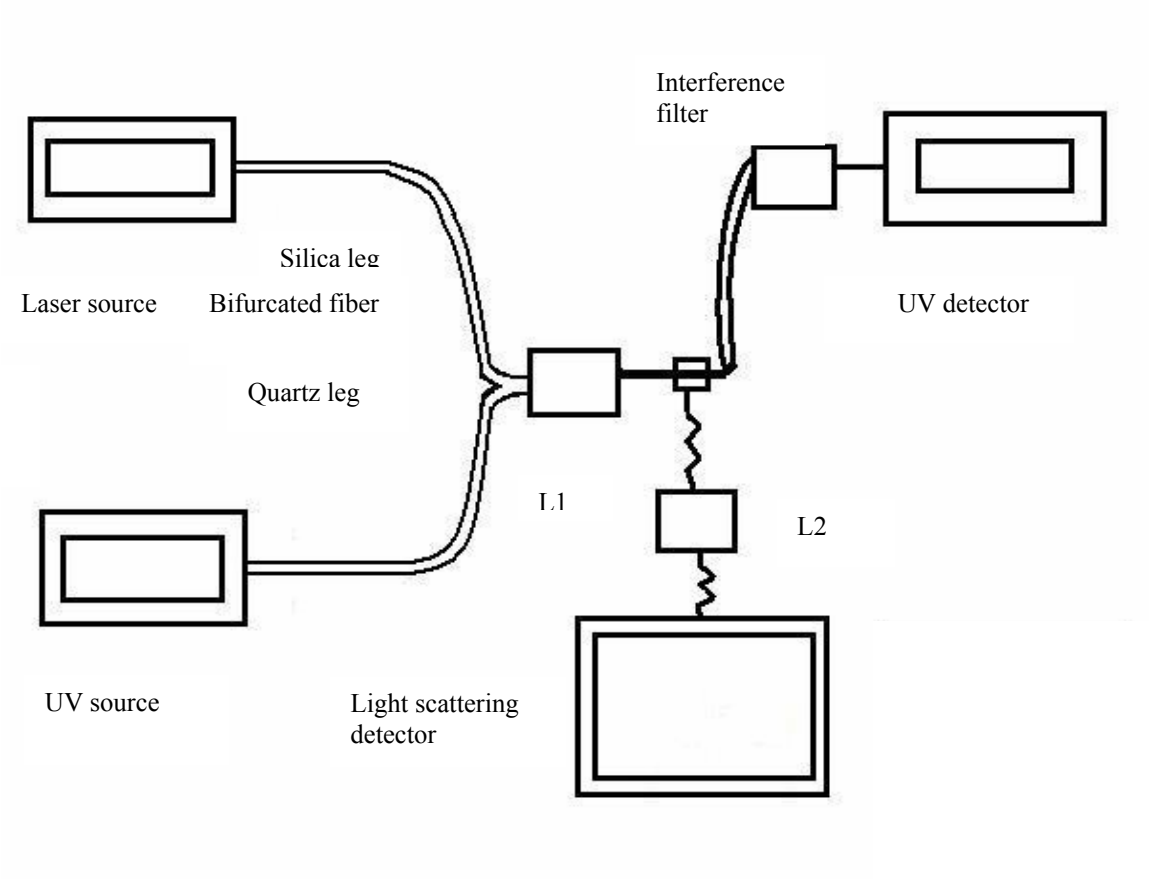

Figure 1: Schematic diagram of scale down static light scattering technique. Here L1 represents a focusing lens and L2 represents a 20X collection lens.

2.5 Self-Interaction Chromatography

From an economic point of view the amount of protein consumed to determine osmotic second virial coefficients using static light scattering, scale down static light scattering and membrane osmometry is fairly large (10).To solve this problem, Tessier, et. al introduced a new form of affinity chromatography called self interaction chromatography. The basic idea of this technique is that the experimental protein is packed on a chromatographic column and then a pulse of the same protein is applied to

calculate retention times which can be linked to the osmotic second virial coefficient using statistical mechanics (8).Tessier calculated the osmotic second virial coefficient using the equation (11)

$$B = (\frac{N_A}{MW^2})(B_{HS} - \frac{k'}{\Phi\rho}) \quad (11)$$

where, B_{HS} =Hard sphere (cm^3) (protein excluded volume)

ρ = Immobilization density (g/cm^3)

Φ = Phase ratio, or the accessible surface area per mobile phase volume

k' = chromatographic capacity factor given by

$$k' = \frac{t_p - t_0}{t_0} \quad (12)$$

where t_p is the time required to elute the protein from the column and t_0 is the dead time or the time to elute a non-interacting molecule (acetone) from the column. This thesis reports osmotic second virial coefficient values for lysozyme using SD/SLS to compare with SIC measurements performed on the same solutions at the University of Alabama at Birmingham.

2.6 Dynamic Light Scattering

Dynamic light scattering measures fluctuations in the average intensity of scattered light arising from different scattering sources. These fluctuations result from the random motion of the protein molecules and are mainly the result of translational and rotational diffusion. This dynamic information is analyzed using a correlator and then

analyzed using various algorithms to extract molecular information. The intensity autocorrelation function is defined for a signal I (t) as

$$G(\tau) = \lim_{T \to \infty} \frac{1}{2T} \int_{-T}^{T} I(t)I(t+\tau)dt \quad (13)$$

Here t is the delay time and I (t + τ) is the signal delayed by a time τ (11)

If we assume a sample containing identical particles, i.e. all these particles have the same shape and size, then the equation 13 can be written as (11,12)

$$G(\tau) = A\,[1 + Be^{-2\Gamma\tau}] \quad (14)$$

where Γ is the decay constant, A is the background and B is a constant depending on the instrument parameters.

For a single diffusing particle

$$\Gamma = Dq^2 \quad (15)$$

and q is the scattering vector given by $4\pi n/\lambda \sin \theta/2$ and D is the translational diffusion coefficient. The Stokes- Einstein equation can be used to estimate the apparent hydrodynamic radius via

$$D = \frac{k_B T}{6\pi\eta R_H} \quad (16)$$

where k_B is the Boltzmann's constant, T is the absolute temperature, η is the viscosity of the solvent in which protein is dissolved, R_h is the apparent hydrodynamic radius of the protein molecule and D is the diffusion coefficient. Generally, larger particles move more slowly and thus have smaller diffusion coefficients compared to smaller particles (12).

Other important parameters that can be assessed in dynamic light scattering are diffusion virial coefficient and polydispersity. One equation frequently used for the concentration dependence of the diffusion coefficient is

$$D = D^0(1+k_D c + ...) \tag{17}$$

where k_D is the diffusion virial coefficient and D^0 is the diffusion coefficient at infinite dilution. The polydispersity value indicates the standard deviation or the spread of the particle sizes about the reported mean radius. The amount of protein consumed for these experiments is always problematic because of high cost and limited availability of protein. In this thesis, a low volume flow cell is used to measure the diffusion virial coefficient of a model protein, lysozyme, and to measure the hydrodynamic radii of monoclonal antibodies.

CHAPTER III

EXPERIMENTAL DESIGN OF A SCALE-DOWN DYNAMIC LIGHT SCATTERING

3.1. Construction of a Scale-Down Dynamic Light Scattering Device

3.1.1 Optical Configuration:

A He-Ne laser of 50mW max output at 632.8nm was employed as a laser source .The laser beam was focused through an attenuator into a low volume flow cell using a collimating lens (Ocean Optics). This collimating lens is placed on a rail and tightly held with the help of metal clamps. It is imperative that the beam passes through the center of the cell and is tightly focused into the cell; otherwise, scattering by the protein solution is not seen by the detector.

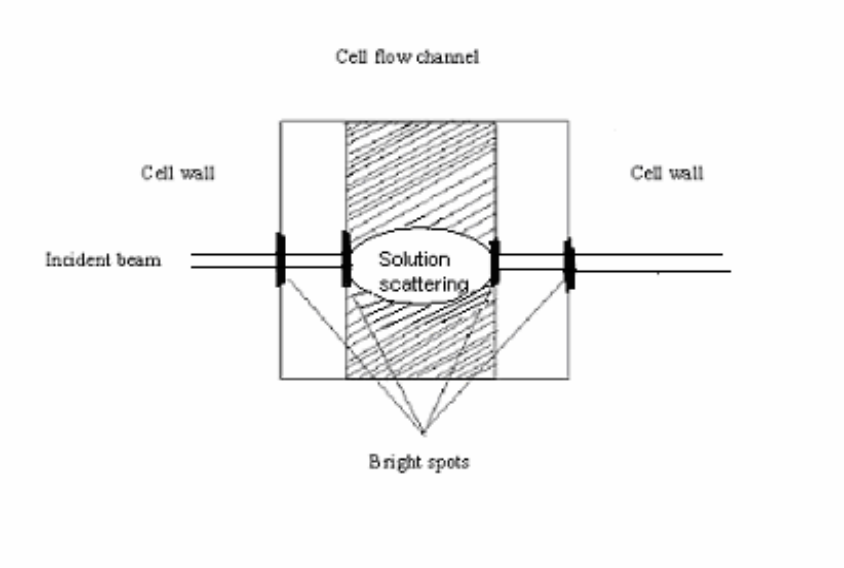

Figure 2: Schematic diagram of the flow cell showing the bright spots at the interfaces

One major problem with this design is the appearance of bright spots on the interface between the center and outside compartments and on the interface between the glass and the air as shown in Figure 2. These bright spots mainly arise because of the change in the refractive indices of the glass/air and glass/water interfaces of the cell. The bright spots act as stray light and mask the true scattering intensity, leading to higher signal and inaccuracies in detection. In order to minimize these bright spots the cell must be regularly cleaned with a soap solution first and then with water at least three times after each experiment. A receiving lens of 20x magnification is placed very near to the cell at an angle of 90^0 in order to focus the image on the detector. In series to the receiving lens, a 0.2 mm pin hole is placed in order to allow only the true solution scattering. This pinhole is positioned at the focal point of the image and an optical fiber FC 200/230 is mounted at the back of the pinhole. Maximum coupling efficiency can be

checked by observing light output at the fiber exit which is connected to a single photon counting module (EG&G optoelectronics, Canada). The signal was directed into a Brookhaven BI2030AT digital correlator and from there it is connected to a computer for the data collection and analysis. A schematic of the scale-down DLS is shown in Figure 3.

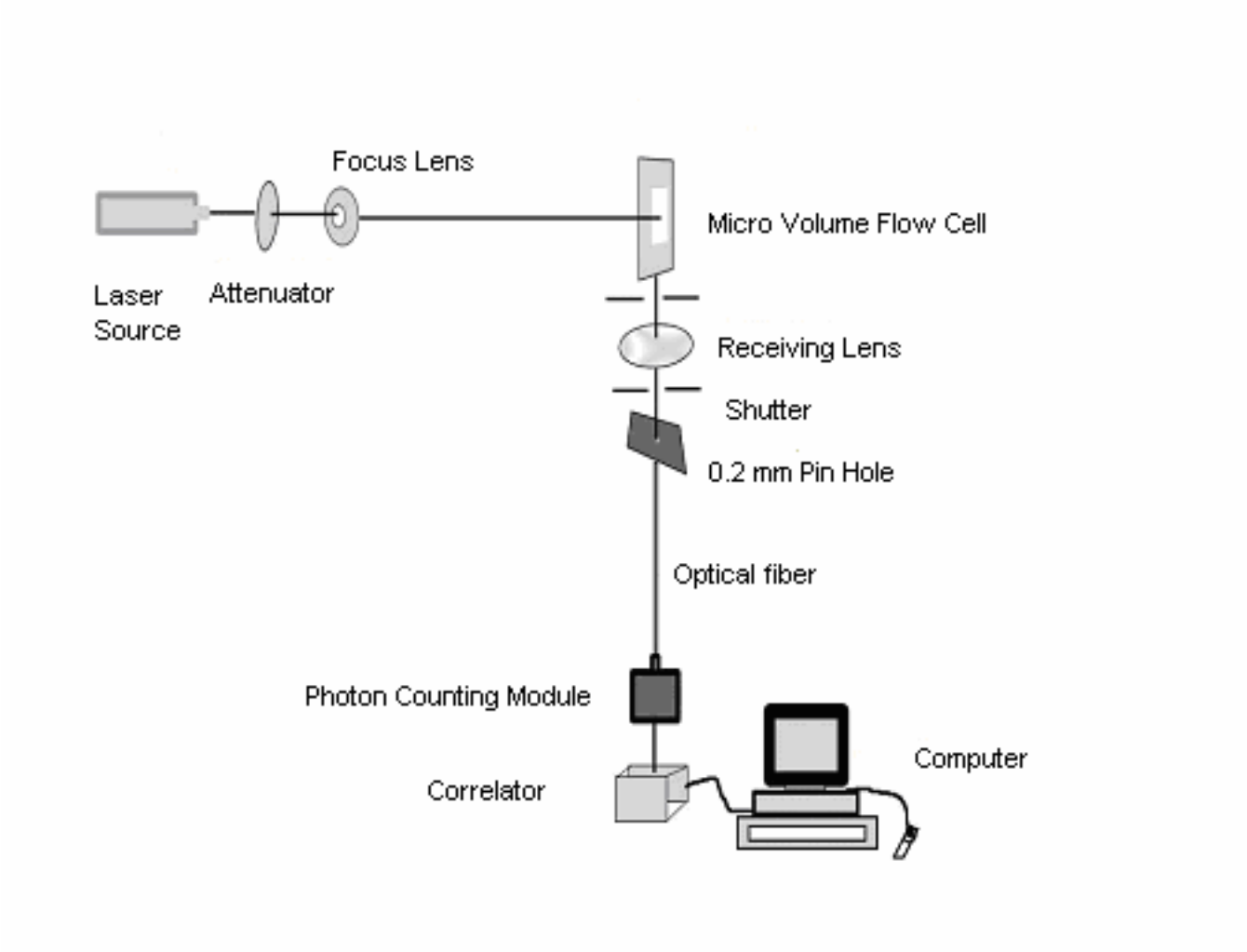

Figure 3: Schematic diagram of the scale-down dynamic light scattering device

3.1.2 Description of the Low Volume Flow Cell

The low volume flow cell from Hellma Cells, Inc. has a 0.25mm cross section channel extending the entire length of the 4.2 x 4.2 x 20.3 mm cell. An aluminum cell holder is utilized to mount the cell on a suitable optical rail. This aluminum cell holder contains a 1/4-28 hole on top and bottom to facilitate inlet and outlets for the sample. Peek tubing of 0.25mm ID is used for both inlets and outlets. The most important feature here is the entire flow path has the same dimensions, 0.25 mm. This helps in reducing the turbulence when the sample enters the low volume flow cell which can some times causes inaccurate measurements.

3.1.3 Flow System Set Up

A flow system was designed to maintain a steady flow of the sample into the cell. This flow system consists of a PHD 4400 programmable syringe pump (Harvard Apparatus, Holliston, MA) which contains an 8 mL stainless steel syringe to maintain continuous buffer supply. The end of this syringe has an Upchurch stainless steel filter to maintain cleanliness of the buffer sample. In series to the syringe is a six port Rheodyne Model 7725i injection valve having a 20 μL loop with another stainless steel Upchurch filter. These stainless steel filters contain a 0.5 μm frit and two 0.2 μm Nucleopore Track Etch membrane filters which are designed to remove unwanted particulates in both buffer solution and the protein sample. A schematic of the flow system is shown in Figure 4.

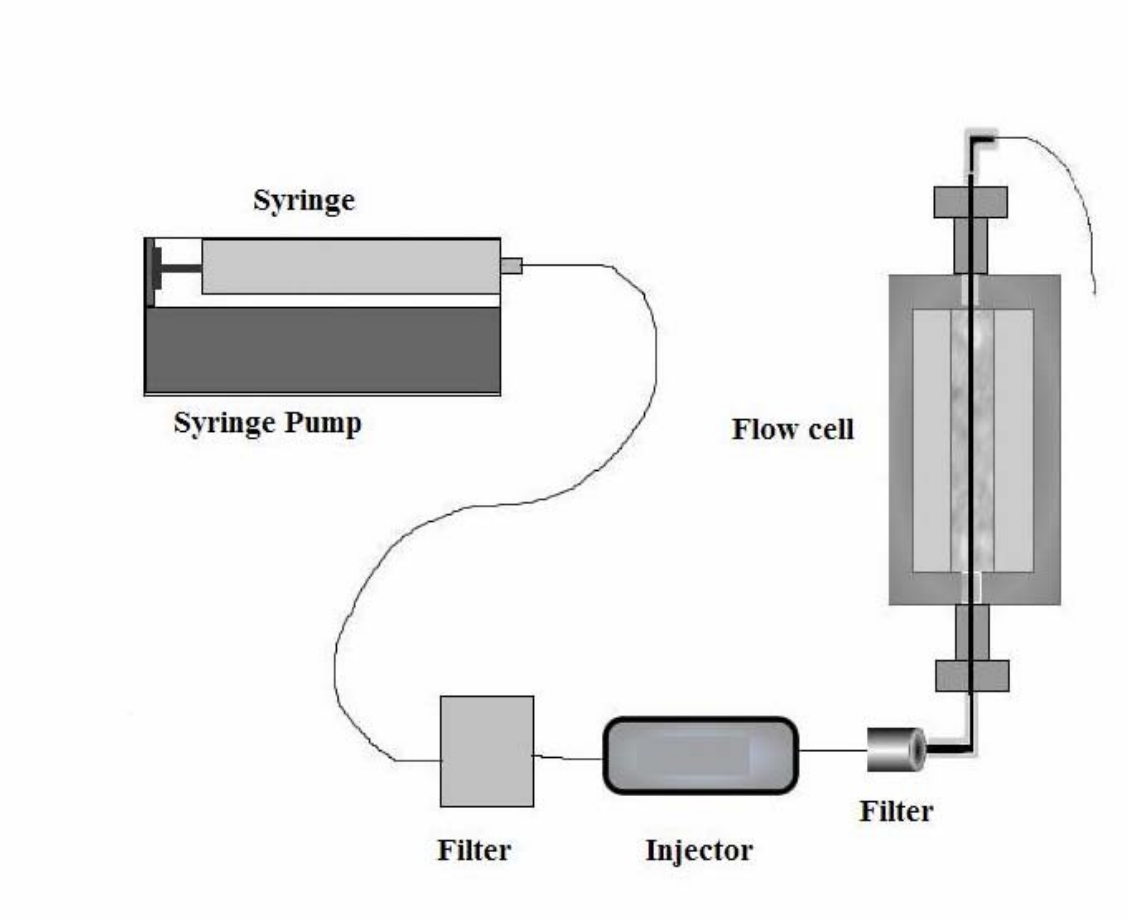

Figure 4: Schematic diagram of the flow injection analysis set up

3.2 Materials and Methods

3.2.1 Chemicals

Glacial acetic acid (17.4 M, Fisher reagent A.C.S), sodium chloride, (Fisher, certified A.C.S), distilled water (Millipore Q Academic), and hen egg white lysozyme obtained from Sigma-Aldrich were used in the validation of the scale-down dynamic light

scattering device. Monoclonal antibodies and their corresponding buffer solutions were obtained from Centocor Pharmaceutical Company (Radnor, PA).

3.2.2 Sample Preparation for Validation of Scale-Down Dynamic Light Scattering Device

The buffer used for validating the scale down dynamic light scattering device was a sodium acetate buffer with 2 % w/v sodium chloride which is prepared by dissolving 6g of glacial acetic acid into a 1L beaker containing 800 mL of distilled water. Sodium chloride (20gms) was added to the 0.1 M HAc to make the desired solution. After this, the pH of the solution was adjusted to 4.2 by titrating with 2 M sodium hydroxide. A lysozyme stock solution of desired concentration was prepared by dissolving an appropriate amount of the protein into the filtered buffer. This stock solution was filtered and checked for its final concentration spectrophotometrically using

$$A=\varepsilon bc \tag{18}$$

For lysozyme A (1 mg/mL, 1 cm, 280 nm) = 2.63 (13).

Serial dilution was performed while measuring the diffusion coefficient of lysozyme at different concentrations from this stock solution. In a similar way all monoclonal antibody protein samples and their experimental buffers were introduced into the low volume flow cell to characterize their hydrodynamic size.

3.2.3 Sample Preparation for Static Light Scattering Experiments

Lysozyme stock solution of about 50 mg/ mL and their respective buffers were delivered from UAB via overnight mail. This highly concentrated stock solution was diluted with a particular experimental buffer and introduced into the sample cell for light scattering measurements as described above.

CHAPTER IV

RESULTS AND DISCUSSION

4.1 Dynamic Light Scattering Experiments

This chapter documents validation of the SD/ DLS using two protein systems 1) lysozyme in 2 % w/v NaCl, and 2) Centocor monoclonal antibodies (mutant and wild type) proteins in their respective formulations.

4.1.1 Demonstration of the Scale-Down Experiment using Lysozyme as a Model Protein

Figure 5 shows the histogram for the particle size distribution of lysozyme in 0.1M NaAc, 2 %(w/v) NaCl, pH 4.2, T=23°C. The hydrodynamic diameter of lysozyme from the SD/DLS measurements is 3.4 nm with a polydispersity of 0.005. X-ray diffraction studies of crystalline lysozyme showed a diameter of 3.44 nm in 0.1M NaAc buffer with 2% (w/v) NaCl, pH=4.2, at T 23°C (14,15,16).This is in excellent agreement with the result from SD/DLS. Muschol and Rosenberger reported a diameter of 3.8nm for lysozyme in NaAc buffer at pH 4.7 in NaCl solution using traditional DLS (17).The good agreement between the SD/DLS and previously reported literature results validated the performance of the SD/DLS experiment.

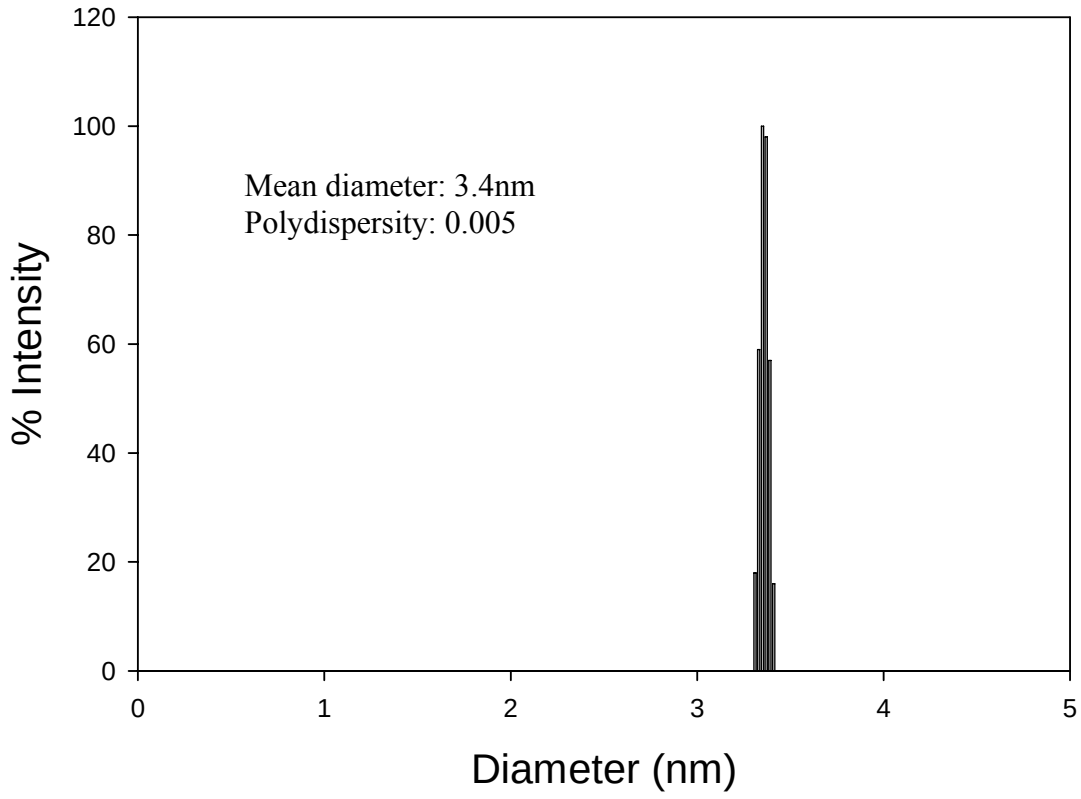

Figure 5: DLS histogram of lysozyme (8mg/ml) in 0.1M NaAc, 2 %(w/v) NaCl, pH 4.2, T=23°C

To further validate the SD/DLS instrument, the translational diffusion coefficients were measured as a function of concentration of lysozyme.

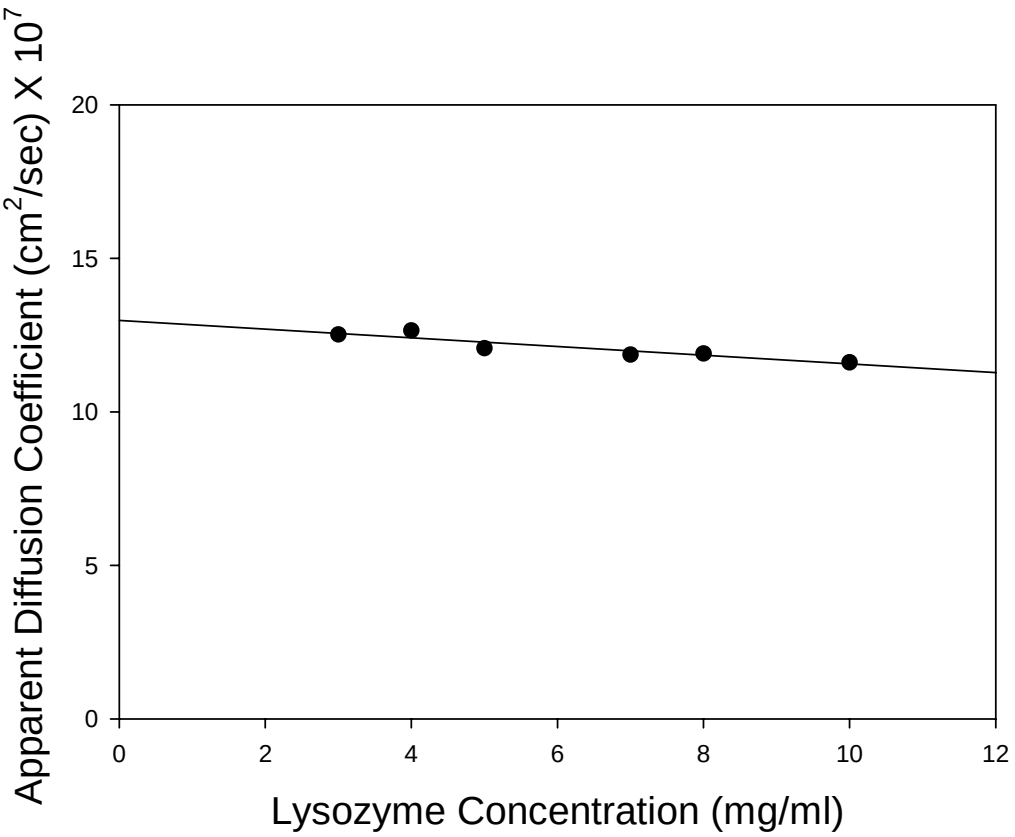

Figure 6: Plot of apparent diffusion coefficient versus lysozyme concentration in 0.1M NaAc buffer with 2% (w/v) NaCl, pH=4.2, T=23°C

From the results shown in the Figure 6, we can conclude that there is little change in the diffusion coefficient as the concentration of the protein is increased up to about 10 mg/ml because hydrodynamic properties of proteins are not expected to vary much in understaurated solutions. The D° value of 12.7x 10^{-7} cm^2/sec and the slope value of -1.37x$10^{-5}$$cm^2$ mL/sec gm gives K_D (diffusion virial coefficient) from equation 17 as -10.7 ml/gm, in reasonable agreement with a reported value of -11.3ml/gm in a similar solution condition (18).

4.1.2 Use of Scale-Down Dynamic Light Scattering Device to Characterize Mutant and Wild Type Proteins

The second system that was chosen to study with the SD/DLS instrument was mutant and wild type proteins obtained from Centocor pharmaceutical company. The hydrodynamic diameters of wild type and mutant proteins were estimated using basic solution theory and compared with those obtained by SD/DLS measurements. The given molecular weight for the wild type and mutant proteins from Centocor was 1.5×10^5 Daltons. An estimate of the hydrodynamic radius for the protein can be made using equation 19(19) where $\overline{V_2}$ is the partial specific volume of the protein (0.72 ml/gm), $\overline{V_1}$ is the partial specific volume of water (1.0 ml/gm), and δ_1 is the hydration (0.37g of water/g of dry protein).

$$V_h = \frac{M}{N}\left[\overline{V_2} + \delta_1\overline{V_1}\right] \tag{19}$$

$$= \frac{1.5\times10^5}{6.023\times10^{23}}\left[\overline{V}_2 + \delta_1\overline{V_1}\right]$$

$$\frac{4}{3}\pi R_H^3 = \frac{1.5\times10^5}{6.023\times10^{23}}\left[\overline{V}_2 + \delta_1\overline{V_1}\right]$$

$$R_H = 4.0\text{nm or } D_H = 8.0\text{nm}$$

The apparent hydrodynamic diameter determined from the SD/ DLS measurements was about 11.2 nm for both wild type and mutant proteins as shown in Figures 7 and 8. This value is considerably larger than that estimated (8.0nm) by using equation 19, which assumes a spherical shape for the protein. All the antibody proteins are expected to possess a prolate/ oblate shape (19) and so generally, the measured diameter is greater

than the calculated diameter due to asymmetry which leads to smaller diffusion coefficients for a given molecular weight of protein. Slight variation can also be expected due to the uncorrected viscosity of the buffer solution at 23.5°C. An important aspect of these results is the very low polydispersity (0.005) obtained for both the wild type and mutant antibodies. Centocor was particularly pleased to learn that their procedures produced this level of homogeneity since that is so important for therapeutic efficacy.

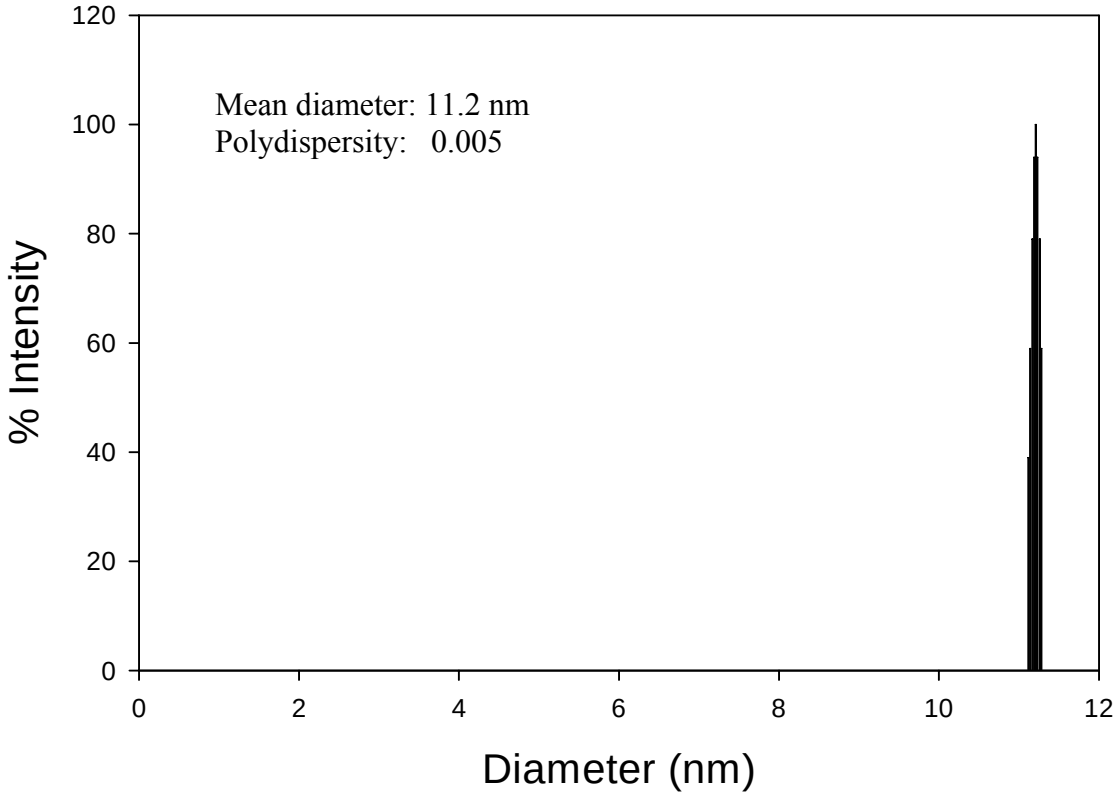

Figure 7: DLS histogram of mutant protein in Centocor buffer, T=23.5°C

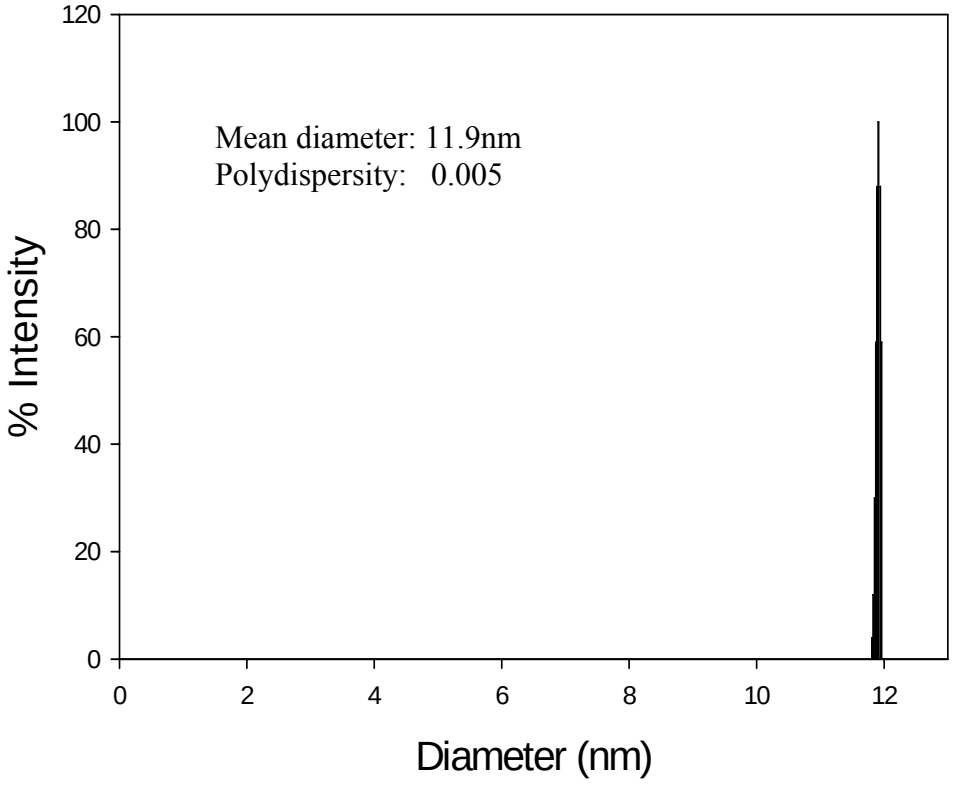

Figure 8: DLS histogram of wild type protein in Centocor buffer, T=23.5°C

4.2 Static Light Scattering Experiments

Osmotic second virial coefficients for lysozyme in ten different crystallization screening solutions were measured using the SD/SLS technique. This work was intended to validate B measurements obtained by self interaction chromatography. The SIC measurements were performed by graduate student David Johnson at the Center for Biophysical Sciences and Engineering at the University of Alabama at Birmingham. An example of the SD/SLS result for solvent 9 is shown in Table 1 while the remaining SD/SLS results are in the appendix. The B value obtained from this experiment was +9.0 mol mL/g^2. A sample chromatogram of solvent 9 using SIC is shown in the Figure 10. Acetone (dark trace) is used as a neutral marker to calculate the dead time required for a noninteracting molecule to pass through the column and the red chromatogram represents the time required to elute protein from the column. A sample calculation of a B value using SIC is shown in Table 12 in the appendix. The shorter retention time of the protein in solvent 9 than that of acetone indicates that the intermolecular forces are repulsive resulting in a positive B value.

Table 1: Light scattering data of lysozyme in solvent 9

Conc. mg/ml	Intensity (mV)	C/(I-S)	Kc/R (mol/g)		
Solvent	800				
1.84	976	1.05E-02	7.31E-05		
1.98	990	1.04E-02	7.29E-05	Operator	Arun
2.31	1018	1.06E-02	7.41E-05	Instrument	SD/SLS
2.70	1050	1.08E-02	7.55E-05	Filters	0.2+0.4µ
2.80	1061	1.07E-02	7.50E-05	Mol. Wt	14,300
3.03	1082	1.07E-02	7.51E-05	A(280,1mg/ml)	2.63
3.38	1114	1.08E-02	7.53E-05	Sample	Lysozyme
3.61	1130	1.09E-02	7.65E-05	Date	July 7-07
3.84	1150	1.10E-02	7.67E-05	Slope	17.2E-04
4.00	1163	1.10E-02	7.71E-05	B(mol·ml/g^2)	8.6E-04
4.17	1180	1.10E-02	7.67E-05		

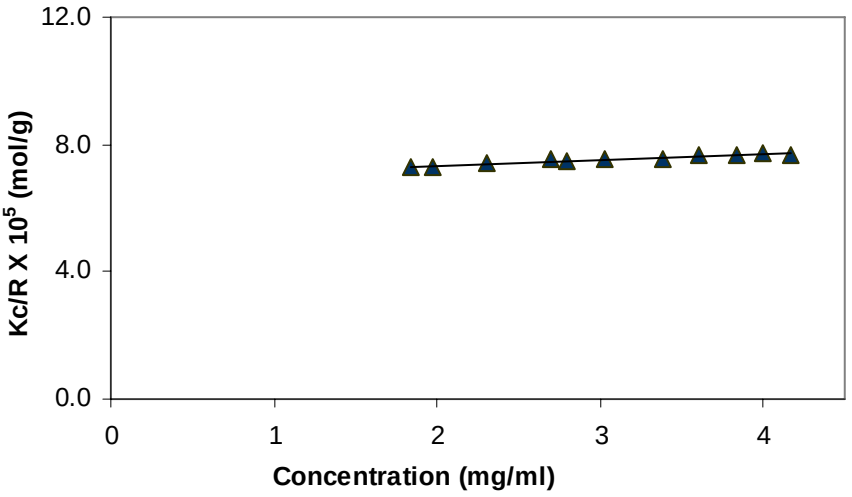

Figure 9: Debye plot for lysozyme in UAB solvent 9, 0.1 M NaAc, 0.3 M NaCl, 0.02 M Arginine, pH 4.76

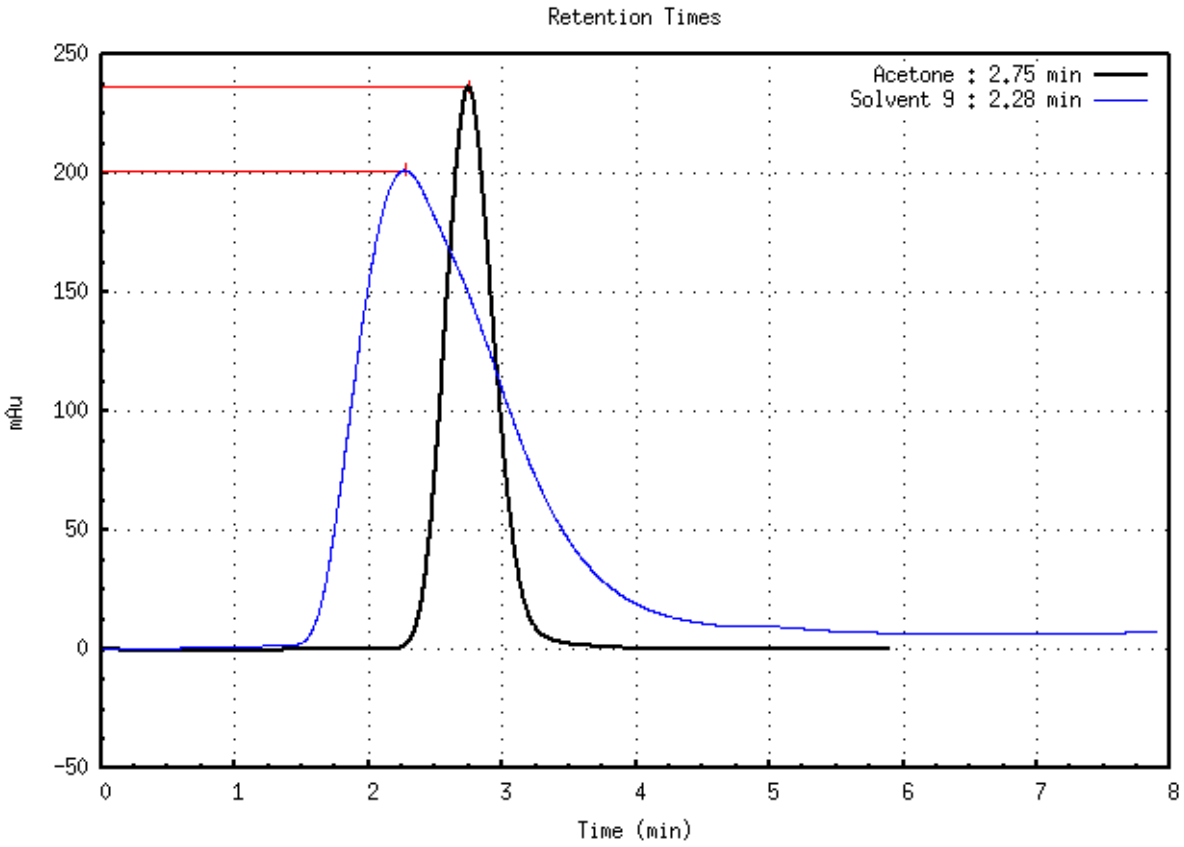

Figure 10: SIC Chromatogram of lysozyme in solvent 9

A summary of the SD/SLS and SIC results is shown in table 2. The solvents studied varied significantly in buffer type, pH, added salt type and concentration, and excipients (amino acids, sugars, e.t.c) type and concentration. Overall the agreement between the SD/SLS and SIC results was satisfactory Correlation between SD/SLS B measurements and SIC B measurements were plotted and shown in the appendix(Figure 20). Some solvents gave essentially the same value for B while others showed variation. The average B values ranged from highly positive (+16 B units) to moderately negative (-

5.5 B units) reflecting protein-solvent interactions dominate in the former case while protein-protein interactions dominate for negative values of B. Notwithstanding two different operators and very two different analytical techniques, the validation of the SIC results by SD/SLS was deemed acceptable. This finding gives confidence that correct estimation of B can be made by SIC. The importance of that finding is that now SIC can be incorporated into a high throughput screening technology that has distinct advantage over SD/SLS. For example, SIC can make a B measurement using only sub-microgram quantities of protein compared to tens of micrograms for SD/SLS. In addition, many screening solvents such as detergents are not appropriate for light scattering because of their excessive background scattering.

Table 2: Average second virial coefficient values for lysozyme in 10 different solvent conditions as determined by both the SLS system and SIC methodology

Solvent	Solvent description	SLS $B*10^4$ mol mL g^{-2}	SIC $B*10^4$ mol mL g^{-2}
9	0.1M NaAc, pH 4.76, 0.3M NaCl,0.02M Arginine	+9.0±1.55	+11
24	0.1M MES, pH 6.1, 0.3 M NaCl, 0.04M Glycine	-1.4±0.01	-1.5
27	0.1 M HEPES, pH 7.48, 0.1M $Na_3C_6H_5O_7$, 0.06M Glycine	+14±0.92	+16
35	0.1 M NaAc, pH 4.76, 0.5 M Na_2SO_4, 0.3 M Sucrose	+9.0±0.55	+8.3
36	0.1 M HEPES, pH 7.48, 0.3 M Na_2SO_4,0.2 M Sucrose	+1.5±0.30	+0.5
39	0.1 M NaAc, pH 4.76, 0.3 M $Na_3C_6H_5O_7$, 0.3 M Mannitol	-1.5±0.41	-1.5
46	0.1 M MES, pH 6.1, 0.3 M $Na_3C_6H_5O_7$, 0.2 M Trehalose	-0.5±0.04	-0.2
60	0.1 M HEPES, pH 4.78, 0.3 M NaCl, 15% MPD	+7.0±0.20	+3.5
72	0.1M NaAc, pH 4.76, 0.1M Na_2SO_4 ,10%Glycerol	+3.7±0.55	+4.8
79	0.1M MES, pH 6.1, 0.5M NaCl,10%PEG4000	-5.0±1.19	-5.5

CHAPTER V

CONCLUSIONS

Light scattering techniques have become invaluable tools in characterizing protein solutions. One light scattering parameter, the osmotic second virial coefficient, reflects protein–protein interactions in dilute solution conditions. Its use has allowed researchers in recent years to determine solution conditions that favor protein crystal growth and formulation conditions that enhance protein shelf life. In addition to the osmotic second virial coefficient, other parameters such as polydispersity and hydrodynamic size also give valuable information regarding protein aggregation. A scale-down dynamic light scattering device was designed to dramatically decrease the amount of the protein expended for these measurements. Using a quartz flow cell with a sample volume of 1μL, the amount of protein required for the SD/DLS experiment was reduced to about 25-50 μg compared to hundreds of micrograms for traditional DLS. The SD/DLS was validated using lysozyme as a model protein system. In addition, the hydrodynamic sizes of monoclonal antibodies were measured using SD/DLS and compared to the theoretical estimates.

The suitability of SIC as a high throughput technique to determine protein-protein interactions was validated using SD/SLS experiments. The amount of the protein and

time expended to measure protein-protein interactions was dramatically reduced using the SIC methodology. The good agreement between the SD/SLS and SIC will encourage the use of SIC as a reliable emerging method to measure osmotic second virial coefficients of proteins.

REFERENCES

(1) W.William Wilson, "Light Scattering as a Diagnostic for Protein Crystal Growth- A Practical Approach", *Journal of Structural Biology*, Vol, 142, 2003, pp. 56-65.

2) P.M.Tessier, A.M.Lenhoff, S.I.Sandler, "Rapid Measurement of Protein Osmotic Second Virial Coefficients by Self-Interaction Chromatography," *Biophysical Journal*, vol.82, **2002**, pp. 1620-1631.

3) George and W.Wilson, "Predicting Protein Crystallization from a Dilute Solution Property," *Acta Cryst.Section* D, Vol.50, **1994**, pp.361-365.

4) P.M.Tessier, A.M.Lenhoff, "Measurements of Protein Self-association as a Guide to Crystallization," Current Opinion in Biotechnology, Vol.14, **2003**, pp. 512-516.

5) T.Ahamed, M.Ottens, G.W.K Van Dedem, and L.A.M. Van der Wielen, "Design of Self-interaction Chromatography as an Analytical tool for Predicting Protein Phase Behavior," *Journal of Chromatography A* , vol. 1089, **2005**, pp.111-124.

6) J.W.Strutt (Lord Rayleigh), "On the Scattering of Light by Small Particles", *Phil.Mag,*Vol 41, **1871**, pp.447-454.

7) B. Guo, S. Kao, H. McDonald, A.Asanov, L.L.Combs, and W.W. Wilson, "Correlation of Second Virial Coefficients and Solubilities useful in Protein Crystal Growth, " *Journal of Crystal growth ,* vol. 196, **1999**, pp.424-423.

8) P.M.Tessier, S.D.Vandrey, B.W.Berger, Rajesh Pazhianur, S.I.Sandler, and A.M.Lenhoff, "Self-interaction Chromatography: A Novel Screening Method for Rational Protein Crystallization", Acta Cryst Section D, Vol. 58, **2002**, pp.1531-1535.

9) A.George, Y.Chiang, B.Guo, A.Arabshashi, Z.Cai, and W.W. Wilson, "Second Virial Coefficient as Predictor in Protein Crystal Growth*",* *Methods in Enzymology*, Vol.276, **1997**,pp100-110.

10) J.C. Fanguy, *The Development of a Scale Down Static Light Scattering Device for Online Determination of the Second Virial Coefficient of Macromolecular Solutions*, doctoral dissertation, Mississippi State University, Mississippi, U.S.A, **2005.**

11) Pecora, R., Ed. Dynamic Light Scattering –Applications of Photon Correlation Spectroscopy, Plenum, New York, **1985**.

12) W.William Wilson, "Monitoring Protein Crystallization Experiments using Dyanmic Light Scattering: Assaying and Monitoring Protein Crystallization in Solution," *Methods*: *A Companion to Methods in Enzymology*, Vol 1, **1990**, pp.110-117.

13) Gerald D.Fasman, "Practical Hand Book of Biochemistry and Molecular Biology, PP 281.

14) V.Mikol, E.Hirsch, and R.Giege, "Diagnostic of Precipitant for Biomacromolecule Crystallization by Quasi-elastic Light-scattering," *J.Mol.Biol*, vol 213, **1990**, pp.187.

15) W. Eberstein, Y.Georgalis, W.Saengar, "Molecular Interactions in Crystallizing Lysozyme Solutions Studied by Photon Correlation Spectroscopy," *Journal of Crystal growth,* Vol.143, **1994**, pp 71-78.

16) D.C.Phillips, *Proc.Nat.Acad.Sci*, U.S.A, Vol.57, **1967**, pp.484-495.

17) M.Muschol, F.Rosenberger, "Interactions in Undersaturated and Supersaturated Lysozyme Solutions, Static and Dynamic Light Scattering Results, *J.Chem.Phys*, Vol.103, **1995**, pp.10424-10432.

18) Y.Chiang, Determination of Diffusion Virial Coefficients and Osmotic Second Virial Coefficients of Lysozyme by Laser Light Scattering, M.S. thesis, Mississippi State, **1994**.

19) M.Sukumar, B.L.Doyle, J.L.Combs and A.H.Pekar," Opalescent Appearance of an IgG1 Antibody at High Concentrations and Its Relationship to Noncovalent Association," *Pharmaceutical Research*, Vol.21, No.7, **2004**, pp. 1087-1093.

(20) Instruction Manual for Model DynaPro 99, Protein Solutions, **1999**.

.

(21) S.B.Dubin, N.A.Clark, G.B.Benedek, *J.Chem.Phys*, Vol.54, **1971**, pp. 5158-5164.

(22) D.E.Kuehner, C.Heyer, C.Ramsch, U.M.Fornefeld, H.W.Blanch, and J.M.Prausnitz, "Interactions of Lysozyme in Concentrated Electrolytes, solutions from Dynamic Light- Scattering Measurements, *Biophysics Journal*, Vol. 73, **1997**, pp. 3211-3224

(23) A.D.Arcy, "Crystallizing Proteins- A Rational Approach," *Acta Cryst Section D*, Vol.50, **1994**, pp.469-471.

APPENDIX

Table 3: Light scattering data of lysozyme in solvent 24

Conc. mg/ml	Intensity (mV)	C/(I-S)	Kc/R (mol/g)		
Solvent	2071				
2.50	2250	1.40E-02	9.77E-05		
2.60	2267	1.33E-02	9.28E-05	Operator	Arun
2.80	2313	1.16E-02	8.09E-05	Instrument	SD/SLS
2.90	2337	1.09E-02	7.62E-05	Filters	0.2+0.4µ
3.40	2349	1.22E-02	8.55E-05	Mol. Wt	14,300
3.88	2385	1.24E-02	8.64E-05	A(280,1mg/ml)	2.63
4.30	2403	1.30E-02	9.06E-05	Sample	Lysozyme
4.74	2439	1.29E-02	9.01E-05	Date	June 8-07
4.90	2463	1.25E-02	8.74E-05	Slope	-2.8E-04
5.00	2478	1.23E-02	8.59E-05	B(mol·ml/g^2)	-1.4E-04
5.50	2521	1.22E-02	8.55E-05		

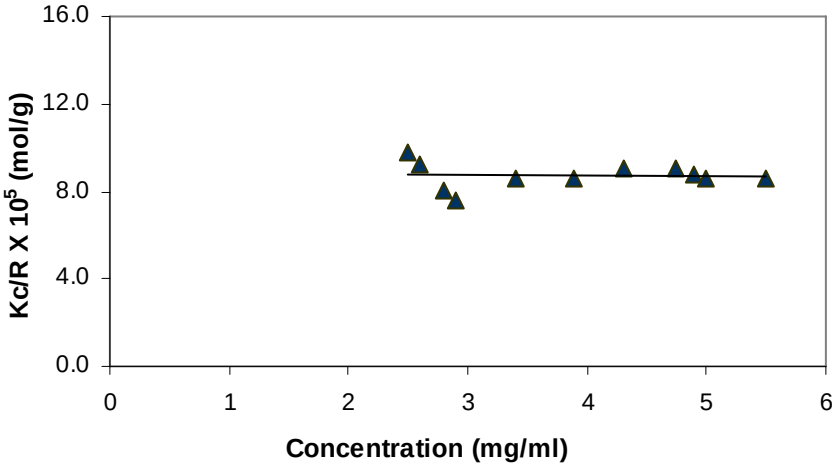

Figure 11: Debye plot for lysozyme in UAB solvent 24, 0.1 M MES, 0.3M NaCl, 0.04 M Glycine, pH = 6.1

Table 4: Light scattering data of lysozyme in solvent 27

Conc. mg/ml	Intensity (mV)	C/(I-S)	Kc/R (mol/g)		
0	918				
1.89	1106	1.01E-02	7.03E-05		
2.02	1118	1.01E-02	7.06E-05	Operator	Arun
2.29	1145	1.01E-02	7.05E-05	Instrument:	SD/SLS
2.46	1163	1.00E-02	7.02E-05	Filters	0.2+0.4µ
2.67	1185	1.00E-02	6.99E-05	Mol. Wt	14,300
2.97	1201	1.05E-02	7.34E-05	A(280,1mg/ml)	2.63
3.29	1226	1.07E-02	7.47E-05	Sample	Lysozyme
3.66	1256	1.08E-02	7.57E-05	Date	July 5-07
3.98	1279	1.10E-02	7.71E-05	Slope	3.6E-03
4.08	1284	1.11E-02	7.80E-05	B(mol·ml/g^2)	1.8E-03
4.20	1299	1.10E-02	7.71E-05		

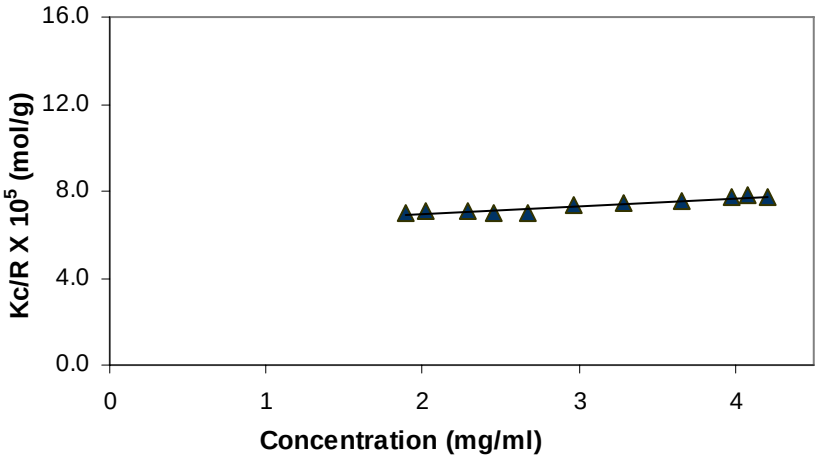

Figure 12: Debye plot for lysozyme in UAB solvent 27, 0.1 M HEPES, 0.1 M $Na_3C_6H_5O_7$, 0.06 M Glycine, pH 4.78

Table 5: Light scattering data of lysozyme in solvent 35

Conc. mg/ml	Intensity (mV)	C/(I-S)	Kc/R (mol/g)		
0	2210				
2.50	2480	9.26E-03	6.48E-05		
2.88	2515	9.44E-03	6.60E-05	Operator:	Arun
3.03	2532	9.41E-03	6.58E-05	Instrument:	SD/SLS
3.38	2566	9.49E-03	6.64E-05	Filters:	0.2+0.4µ
3.85	2612	9.58E-03	6.70E-05	Mol. Wt	14,300
4.01	2626	9.64E-03	6.74E-05	A(280,1mg/ml)	2.63
4.29	2655	9.64E-03	6.74E-05	Sample	Lysozyme
4.54	2677	9.72E-03	6.80E-05	Date	July 3 -07
4.77	2696	9.81E-03	6.86E-05	Slope	13.6E-04
5.10	2726	9.88E-03	6.91E-05	B(mol·ml/g^2)	6.8E-04
5.30	2753	9.76E-03	6.83E-05		

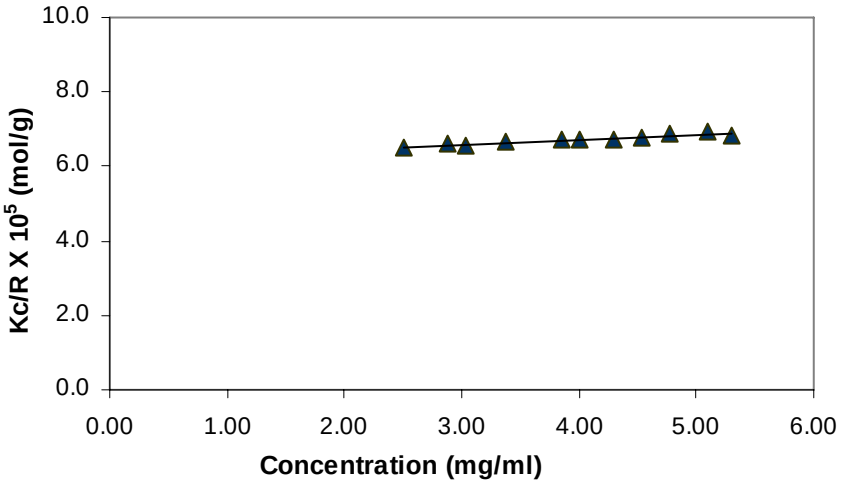

Figure 13: Debye plot for lysozyme in UAB solvent 35, 0.1 M Na_2SO_4, 0.3 M Sucrose, pH 4.76

Table 6: Light scattering data of lysozyme in solvent 36

Conc. mg/ml	Intensity (mV)	C/(I-S)	Kc/R (mol/g)		
Solvent	2412				
1.86	2475	2.95E-02	2.06E-04		
2.00	2480	2.94E-02	2.06E-04		
2.50	2498	2.91E-02	2.03E-04	Instrument	SD/SLS
2.88	2514	2.82E-02	1.97E-04	Filters	0.2+0.4µ
3.38	2522	3.07E-02	2.15E-04	Mol. Wt	14,300
3.59	2534	2.94E-02	2.06E-04	A(280,1mg/ml)	2.63
3.91	2540	3.05E-02	2.14E-04	Sample	Lysozyme
4.42	2548	3.25E-02	2.27E-04	Date	July 1-07
4.70	2560	3.18E-02	2.22E-04	Slope	2.8E-04
5.04	2583	2.95E-02	2.06E-04	B(mol·ml/g^2)	1.4E-04
5.27	2615	2.60E-02	1.82E-04		

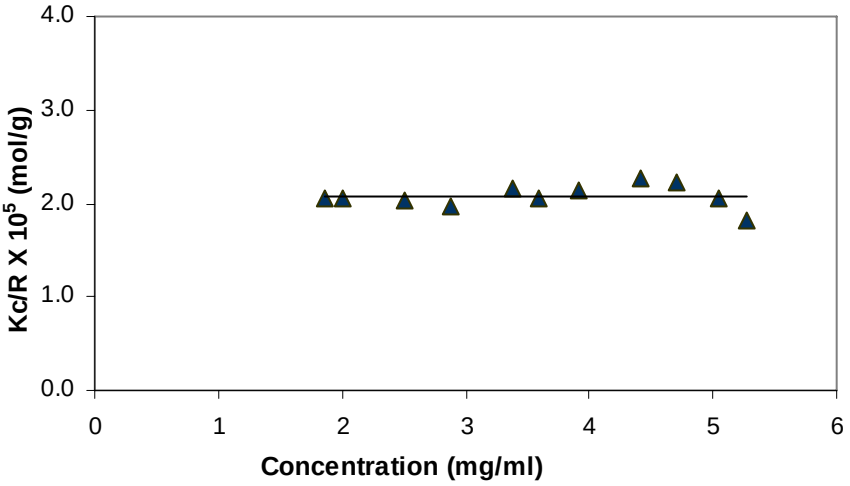

Figure 14: Debye plot for lysozyme in UAB solvent 36, 0.1 M HEPES, 0.1 M Na_2SO_4, 0.3 M Sucrose, pH 7.48

Table 7: Light scattering data of lysozyme in solvent 39

Conc. mg/ml	Intensity (mV)	C/(I-S)	Kc/R (mol/g)		
Solvent	1858				
2.45	2106	9.88E-03	6.91E-05		
2.86	2148	9.86E-03	6.90E-05	Operator	Arun
3.05	2178	9.53E-03	6.67E-05	Instrument	SD/SLS
3.21	2186	9.79E-03	6.84E-05	Filters	0.2+0.4µ
3.38	2198	9.94E-03	6.95E-05	Mol. Wt	14,300
3.52	2219	9.75E-03	6.82E-05	A(280,1mg/ml)	2.63
3.78	2244	9.79E-03	6.85E-05	Sample	Lysozyme
				Date	Jun 23-07
				Slope	-2.2E-04
				B(mol·ml/g^2)	-1.1E-04

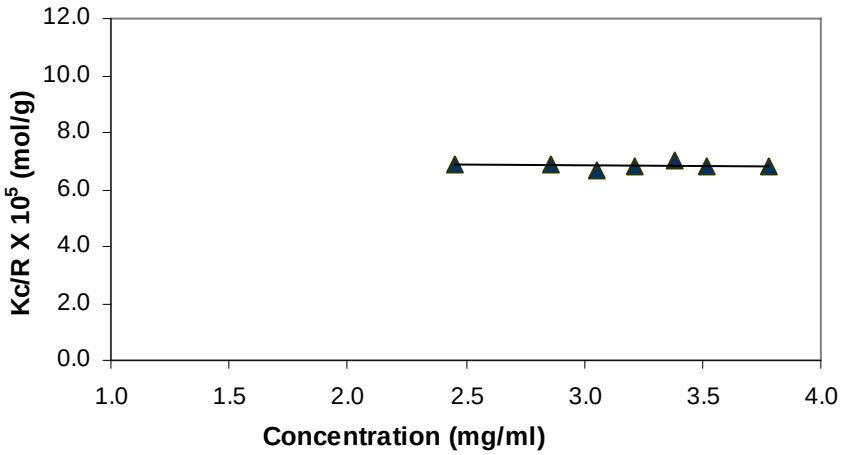

Figure 15: Debye plot for lysozyme in UAB solvent 39, 0.1 M NaAc, 0.3 M $Na_3C_6H_5O_7$, 0.3 M Mannitol, pH 4.76

Table 8: Light scattering data of lysozyme in solvent 46

Conc. mg/ml	Intensity (mV)	C/(I-S)	Kc/R (mol/g)		
Solvent	629				
1.73	824	8.87E-03	6.20E-05		
2.24	877	9.03E-03	6.32E-05	Operator	Arun
2.54	904	9.24E-03	6.46E-05	Instrument	SD/SLS
2.78	934	9.11E-03	6.37E-05	Filters	0.2+0.4µ
3.06	969	9.00E-03	6.29E-05	Mol. Wt	14,300
3.27	990	9.06E-03	6.33E-05	A(280,1mg/ml)	2.63
3.38	995	9.23E-03	6.46E-05	Sample	Lysozyme
3.6	1013	9.38E-03	6.56E-05	Date	Jun 20-07
3.95	1071	8.94E-03	6.25E-05	Slope	-10.7E-05
4.12	1089	8.96E-03	6.26E-05	B(mol·ml/g^2)	-5.38E-05
4.42	1128	8.86E-03	6.19E-05		

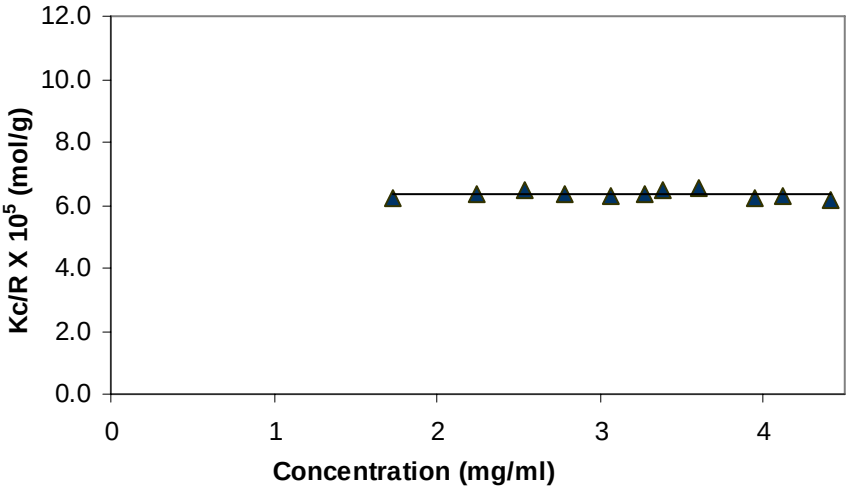

Figure 16: Debye plot for lysozyme in UAB solvent 46, 0.1 M MES, 0.3 M Citrate, 0.2M Trehalose, pH 6.1

Table 9: Light scattering data of lysozyme in solvent 60

Conc. mg/ml	Intensity (mV)	C/(I-S)	Kc/R (mol/g)		
Solvent	2174				
2.53	2356	1.39E-02	9.72E-05		
2.79	2372	1.41E-02	9.85E-05	Operator	Arun
2.94	2390	1.36E-02	9.52E-05	Instrument:	SD/SLS
3.25	2410	1.38E-02	9.63E-05	Filters:	0.2+0.4µ
3.53	2432	1.37E-02	9.57E-05	Mol. Wt	14,300
3.87	2457	1.37E-02	9.56E-05	A(280,1mg/ml)	2.63
4.53	2486	1.45E-02	1.02E-04	Sample	Lysozyme
4.87	2511	1.45E-02	1.01E-04	Date	June 17-07
5.04	2520	1.46E-02	1.02E-04	Slope	14.0E-04
5.24	2538	1.44E-02	1.01E-04	B (mol·ml/g^2)	7.0E-04
5.63	2579	1.39E-02	9.72E-05		

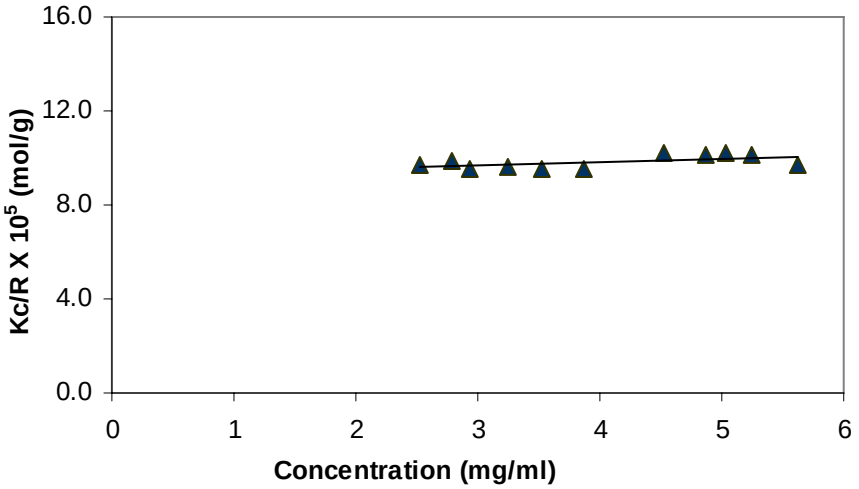

Figure 17: Debye plot for lysozyme in UAB solvent 60, 0.1 M HEPES, 0.3 M NaCl, 15% MPD, pH 4.78

Table 10: Light scattering data of lysozyme in solvent 72

Conc. mg/ml	Intensity (mV)	C/(I-S)	Kc/R (mol/g)		
Solvent	805				
1.27	923	1.08E-02	7.53E-05		
1.48	942	1.08E-02	7.55E-05		
1.71	964	1.08E-02	7.52E-05	Instrument:	SD/SLS
2.11	1003	1.07E-02	7.45E-05	Filters:	0.2+0.4µ
2.52	1037	1.09E-02	7.60E-05	Mol. Wt	14,300
3.02	1082	1.09E-02	7.62E-05	A(280,1mg/ml)	2.63
3.73	1141	1.11E-02	7.76E-05	Sample	Lysozyme
4.42	1203	1.11E-02	7.77E-05	Date	June 15-07
4.79	1228	1.13E-02	7.92E-05	Slope	11.0E-04
5.31	1269	1.14E-02	8.00E-05	B(mol·ml/g^2)	5.5E-04
5.64	1305	1.13E-02	7.89E-05		

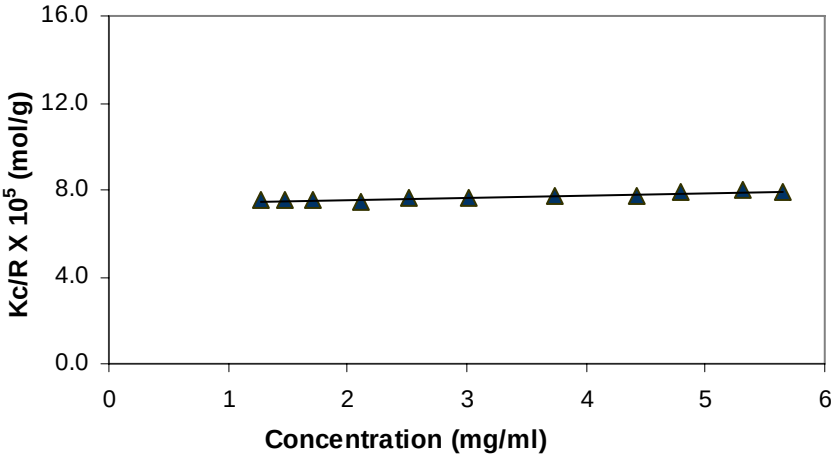

Figure 18: Debye plot for lysozyme in UAB solvent 72, 0.1 M NaAc, 0.1 M Na_2SO_4 10 % Glycerol, pH= 4.76

Table 11: Light scattering data of lysozyme in solvent 79

Conc. mg/ml	Intensity (mV)	C/(I-S)	Kc/R (mol/g)		
Solvent	810				
1.51	956	1.03E-02	7.71E-05		
1.75	974	1.07E-02	6.55E-05		
2.09	1008	1.06E-02	6.48E-05	Operator	Arun
2.42	1027	1.12E-02	6.85E-05	Instrument	SD/SLS
2.67	1045	1.14E-02	6.98E-05	Filters	0.2+0.4
2.82	1061	1.12E-02	6.90E-05	Mol. Wt	14,300
3.35	1114	1.10E-02	6.77E-05	A(280,1mg/ml)	2.63
3.75	1168	1.05E-02	6.43E-05	Sample	Lysozyme
3.97	1204	1.01E-02	6.19E-05	Date	July 8-07
4.03	1215	9.95E-03	6.11E-05	Slope	-16.3E-04
4.05	1225	9.76E-03	5.99E-05	B(mol·ml/g^2)	-8.18E-04

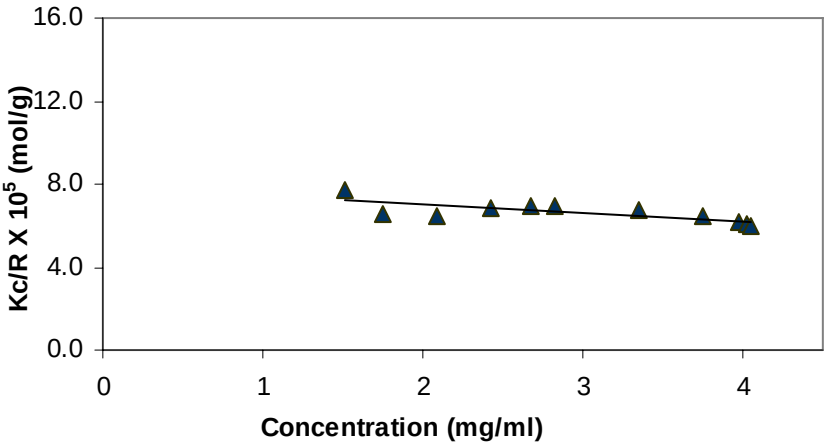

Figure 19: Debye plot for lysozyme in UAB solvent 79, 0.1 M MES, 0.5M NaCl, 10% PEG 4000, pH 6.1

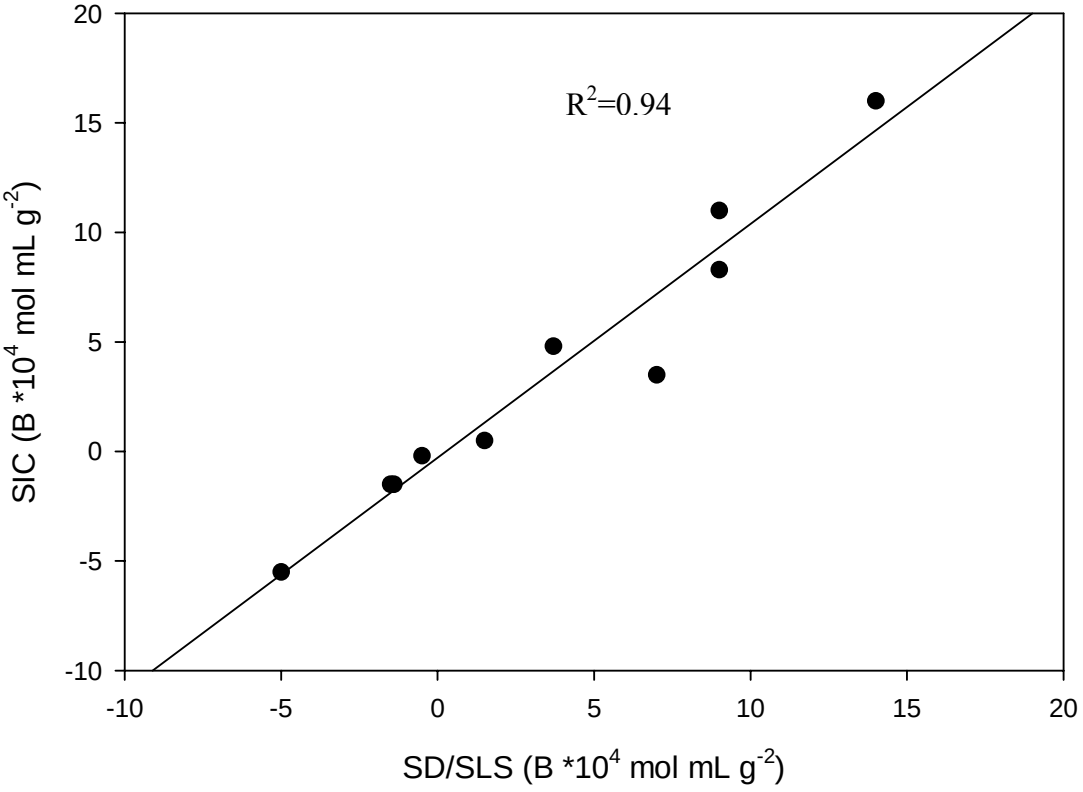

Figure 20: Correlation of B values measured by SD/SLS with B values measured using SIC

Table 12: Key parameters for calculating an osmotic second virial coefficient for lysozyme using self interaction chromatography

Parameter	Description	Value
MW	Molecular weight (Daltons)	14,300 g/mol
k'	Retention factor	-0.17
Φ	Accessible surface area /mobile phase volume for r=4.06nm	16.0m^2/ml
ρ	Immobilization density (amount of the protein immobilized per unit surface area)	6.221×10^{16} mg/ml
B_{HS}	Excluded volume	6.24×10^{-20} cm^3
t_p	Retention time of protein	2.28min
t_0	Retention time of acetone	2.75 min

$$k' = \frac{t_p - t_0}{t_0} \qquad B = B_{HS} - \frac{k'}{\Phi \ \rho} \times \frac{N_A}{MW^2}$$

$$= \frac{2.28 - 2.75}{2.75} = -0.17 \qquad = +6.8 \text{ mol ml } g^{-2}$$